Proc. Roy. Soc. A. **305**, 235–250 (1968)
Printed in Great Britain

The propagation of continental shelf waves

By V. T. Buchwald† and J. K. Adams
Department of Applied Mathematics, University of Sydney, Australia

(*Communicated by M. S. Longuet-Higgins, F.R.S.—Received* 24 *October* 1967)

Taking the case of a continental shelf of exponential slope, and assuming zero horizontal divergence, the authors derive a simple theory of free shelf waves, which, however, is more general than previous theories in that shorter as well as longer waves (in comparison with previous work) are taken into account. The properties of the waves are discussed, and the dispersion curves for each mode are obtained. Although the phase velocities of shelf waves are always in the same sense as those of Kelvin waves, there is a negative group velocity for a range of wavelengths, indicating that energy can propagate in the opposite sense.

A similar approach is used to derive a theory for free waves propagating on a shelf between two regions of constant depth. The limiting case of a shelf of zero width is also considered, and is compared with a limiting case of the 'double-Kelvin' waves discovered by Longuet-Higgins (1967).

1. Introduction

At the low frequencies associated with barometric pressure changes due to weather systems, the theoretical 'isostatic' response of an ocean of uniform depth is that of an inverse barometer, in the sense that records should show a rise in sea level of −1·01 cm for each millibar rise in atmospheric pressure. However, in examining the relation between sea level and pressure at a number of Australian stations, Hamon (1962, 1963, 1966) has shown that on the east and west coasts the response is not isostatic. For instance, averaged over various periods of some months, the regression coefficient in Sydney of sea level on pressure was found to be between −0·35 and −0·52 cm/mb, while in Coff's Harbour the regression coefficient was even smaller in magnitude. Similar calculations for the west coast showed a regression coefficient of about −1·8 cm/mb in Fremantle, but at Hobart in Tasmania and at Lord Howe Island there was no significant departure from the theoretical isostatic behaviour.

The anomalous behaviour observed by Hamon has been attributed by Robinson (1964) to the presence of 'shelf waves' which are generated in some way by weather systems. In his model, Robinson assumed a shallow shelf of constant slope and width, bounded at the edge by a sudden drop to a deep ocean of uniform depth. For periods which are long in comparison with the pendulum-day, Robinson showed that, assuming wavelengths large compared with the width of the shelf, the equations of motion can be reduced to a Bessel's equation. Satisfaction of appropriate boundary conditions at the edge of the shelf (i.e. continuity of pressure and normal mass flux) results in a frequency relation which predicts that an infinite number of modes of very long waves of the second class can propagate freely without dispersion in one direction along the shelf. Just as for Kelvin waves, for which the solid boundary is to the right of the direction of propagation in the Northern hemisphere, and to the left in the Southern hemisphere, long shelf waves would be expected to travel in an anticlockwise sense around the Australian coast. Myzak (1967) has calculated

† Now at School of Mathematics, University of New South Wales.

the effects of stratification, deep sea currents, and finite edge slope on Robinson's model. He showed that taking these effects into account can cause important changes in the numerical results, but that the general conclusions are not changed significantly.

The main drawback of Robinson's model is that, in order to achieve necessary simplicity, only very long waves are considered, so that, as it turns out, most of the interesting modal structure of shelf waves is neglected. In this paper we use a model in which the shelf has an exponential slope from shallow water to deep ocean. It will be shown that for the appropriate length and time scale the assumption of zero horizontal divergence is a very good approximation, and in this case the exponential shelf model leads to very simple equations which take into account shorter waves as well as the very long ones. The waves prove to be highly dispersive in general, and, although the phase velocity is always in the same sense as the Kelvin wave velocity, the group velocity changes sign so that energy can be propagated in the opposite sense. There is a form of resonance in each mode at the frequency at which the group velocity is zero, and this frequency is also the maximum frequency for which the mode exists. For any given frequency only a finite number of propagating modes are possible.

Shelf waves can also occur on shelves in the deep ocean. Taking as a model the case of a shelf of exponential slope and constant width between two infinite oceans of uniform depth, a theory similar to that of continental shelf waves is derived. Although the resulting frequency equations are a little more complicated than in the previous case, the dispersion curves are much the same. Again there is a maximum frequency in each propagating mode, and the group velocity changes sign at this maximum, so that to each given frequency there correspond two wavelengths. The energy associated with the longer waves propagates in the sense of Kelvin waves in the deeper ocean, and that associated with the shorter waves travels in the opposite sense. It is also possible to make the shelf width tend to zero, keeping the depths of the oceans constant. In this limiting case of a sudden discontinuity in depth, the condition that mass flux along the shelf is zero must be applied, with the result that waves along the discontinuity are possible only for a fixed frequency. However, the wavelengths of these waves decrease with the shelf width, so that the phase and group velocities also become zero. It should be noted that this degenerate case is also the non-divergent limit of the 'double-Kelvin' waves discovered by Longuet-Higgins (1968).

This paper is concerned only with the properties of freely propagating waves. Robinson (1964) and Myzak (1967) have suggested that their generation is due to resonance with pressure, but the authors consider that it is more likely that the waves are forced by the surface stress due to the geostrophic wind. Although a brief, qualitative, account is given at the end of this paper, it is hoped that the question of how shelf waves are generated will be fully discussed in a later publication.

2. The equations of motion

When referred to horizontal rectangular coordinates x, y, the equations of motion in the linearized shallow-water wave theory are

$$\frac{\partial u}{\partial t} - fv = -g\frac{\partial \zeta}{\partial x}, \tag{2·1}$$

$$\frac{\partial v}{\partial t} + fu = -g\frac{\partial \zeta}{\partial y}, \tag{2·2}$$

and the equation of continuity is

$$\frac{\partial (hu)}{\partial x} + \frac{\partial (hv)}{\partial y} + \frac{\partial \zeta}{\partial t} = 0. \tag{2·3}$$

In these equations, ζ is the elevation of the free surface above the equilibrium level, $h(x, y)$ is the depth, u and v, are the components of the velocity in the x, y directions, g is the acceleration due to gravity, and f is the Coriolis parameter, given by $f = 2\Omega \sin\theta$, where Ω is the Earth's angular velocity and θ is the latitude.

It is convenient at this stage to make two important approximations. First, it will be assumed that

$$f = \text{const.} \tag{i}$$

Longuet-Higgins (1964, 1965) has shown that it is reasonable to account for the variation of f with latitude by making the assumption $\partial f/\partial y = \beta$, where β is a constant, and the y axis points north. We shall be considering periods of about 1 to 10 days, and shelf widths of the order of 100 km. It is generally true that for these length and time scales it is possible to neglect the β terms in the equations of motion, compared with variations in depth which are sufficiently sharp. It could, perhaps, be argued that there is another length scale given by the wavelength of the shelf waves, and if this is large then the β terms will be comparable with other terms in the equations. Whilst this assertion is correct, it turns out that these latter terms are sufficiently small to be themselves neglected, so that (i) remains a good approximation. The actual effect of retaining the terms in β is examined in the appendix, in which it is shown that for the shelf model under consideration these terms are, in fact, negligible in a first order theory.

Secondly, we shall assume that the periods of the phenomena under examination are greater than $2\pi/f$, and that

$$\epsilon = \frac{f^2 L^2}{g h_0} \ll 1, \tag{ii}$$

where L is the shelf width, and h_0 is the depth, averaged in some way. For the Australian coast, ϵ is less than 5×10^{-2}, which certainly satisfies (ii). If we eliminate u, v, from equations (2·1) to (2·3) then it can be shown that if $\epsilon = 0$ then it is the third term of (2·3) which vanishes. The motion is then horizontally non-divergent with

$$\frac{\partial (hu)}{\partial x} + \frac{\partial (hv)}{\partial y} = 0 \tag{2·4}$$

replacing (2·3). It is now possible to express u, v in terms of a stream function ψ by

$$u = D\frac{\partial \psi}{\partial y}, \quad v = -D\frac{\partial \psi}{\partial x}, \tag{2·5}$$

so that (2·4) is satisfied when $D = h^{-1}$.

Differentiating (2·1) partially with respect to y, (2·2) with respect to x, subtracting, and using (2·5), the vorticity equation

$$\frac{\partial}{\partial t}\left[\frac{\partial}{\partial x}\left(D\frac{\partial \psi}{\partial x}\right) + \frac{\partial}{\partial y}\left(D\frac{\partial \psi}{\partial y}\right)\right] + f\left(\frac{\partial D}{\partial y}\frac{\partial \psi}{\partial x} - \frac{\partial D}{\partial x}\frac{\partial \psi}{\partial y}\right) = 0, \tag{2·6}$$

is obtained.

3. The shelf model

Suppose we have a straight coast-line bounding a semi-infinite ocean, and choose axes as in figure 1, the y axis being along the coast, and the x axis normal to it.

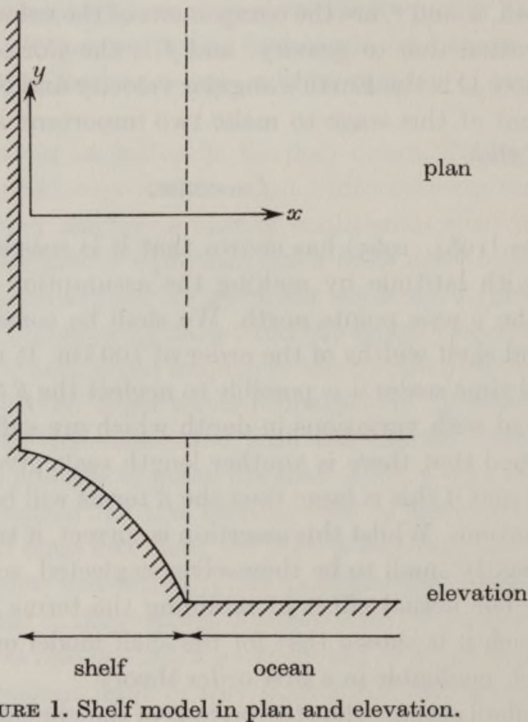

Figure 1. Shelf model in plan and elevation.

Without loss of generality it is possible to choose units such that the shelf occupies the strip $0 < x < 1$, and suppose that the ocean $x > 1$ has constant depth. Assume that the profile of the shelf region is independent of y, and that the inverse depth is given by

$$\begin{aligned} D(x) &= D_0 e^{-2bx} \quad (0 < x < 1) \\ &= D_1 \quad (x > 1), \end{aligned} \tag{3·1}$$

where $D_1 = D_0 e^{-2b}$, so that $D(x)$ is continuous at $x = 1$. Appropriate values of the constants for the shelf near Sydney are

$$D_0 = 1{\cdot}5 \times 10^{-4}\,\text{cm}^{-1}, \quad D_1 = 2 \times 10^{-6}\,\text{cm}^{-1}, \quad \text{and} \quad b = 2{\cdot}7.$$

The shelf width is taken to be 80 km, which is now the unit of length. The resulting model of the shelf is illustrated in figure 2, in which it is compared with measurements of the actual topography.

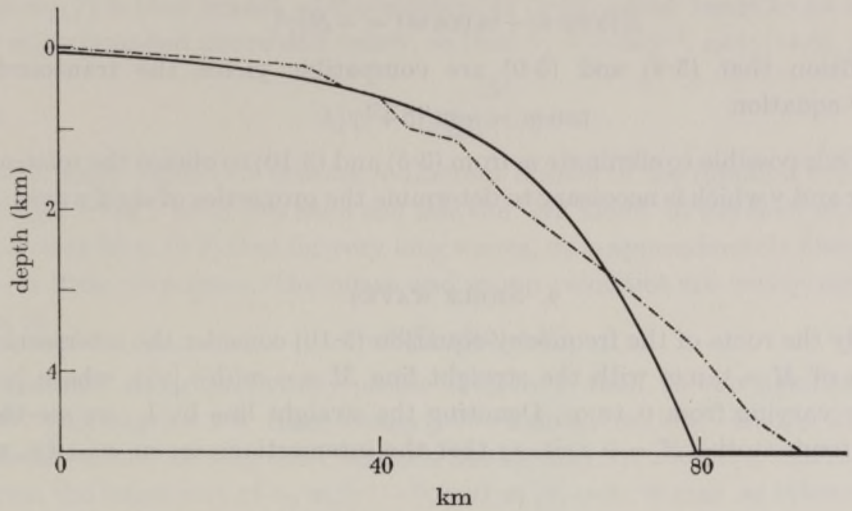

FIGURE 2. Comparison of the bottom topography (–·–·) near Sydney with theoretical model (——).

For free waves assume that

$$\psi(x, y, t) = \Phi(x)\, e^{i(\gamma y - \omega t)}, \tag{3·2}$$

so that, in the shelf region, substitution of (3·1) and (3·2) in (2·6) yields, after a little algebra,

$$\frac{d^2\Phi}{dx^2} - 2b\frac{d\Phi}{dx} - \left(\frac{2b\gamma}{\sigma} + \gamma^2\right)\Phi = 0, \tag{3·3}$$

where $\sigma = \omega/f$.

The boundary condition at $x = 0$ is that $u = 0$, which is satisfied by taking $\Phi(0) = 0$. Hence the solution of (3·3) appropriate to the shelf region is

$$\Phi_s = A\, e^{b(x-1)} \sin mx, \tag{3·4}$$

where A is an arbitrary constant, and m is given by

$$m^2 + \gamma^2 + b^2 + 2b\gamma/\sigma = 0. \tag{3·5}$$

It follows immediately from this relation that γ/σ is negative. In the Northern hemisphere $f > 0$, so that $c = \omega/\gamma$ is negative and waves propagate with phase velocities in the negative y direction only. In the Southern hemisphere $f < 0$, and the phase velocities are in the positive y direction.

In the deep ocean $b = 0$, and the appropriate solution of (3·3) which is not large at infinity is

$$\Phi_0 = B\, e^{-|\gamma|(x-1)}, \tag{3·6}$$

where B is a constant. At $x = 1$, ζ and u are continuous, which implies that

$$\left.\begin{aligned} \Phi_s(1) &= \Phi_0(1), \\ \text{and} \quad \Phi_s'(1) &= \Phi_0'(1). \end{aligned}\right\} \tag{3·7}$$

From (3·4), (3·6) and the first of (3·7),

$$A \sin m = B, \tag{3·8}$$

while, from the second of (3·7),

$$A(b \sin m + m \cos m) = -B|\gamma|. \tag{3·9}$$

The condition that (3·8) and (3·9) are compatible yields the transcendental frequency equation

$$\tan m = -m/(b+|\gamma|). \tag{3·10}$$

In theory it is possible to eliminate m from (3·5) and (3·10) to obtain the relationship between σ and γ which is necessary to determine the properties of shelf waves.

4. Shelf waves

To study the roots of the frequency equation (3·10) consider the intersections of the graph of $M = \tan m$ with the straight line $M = -m/(b+|\gamma|)$, where $|\gamma|$ is a parameter varying from 0 to ∞. Denoting the straight line by l_γ, we see that as $\gamma \to \infty$, l_γ tends to the $M = 0$ axis, so that the intersections are at $m = k\pi$, where

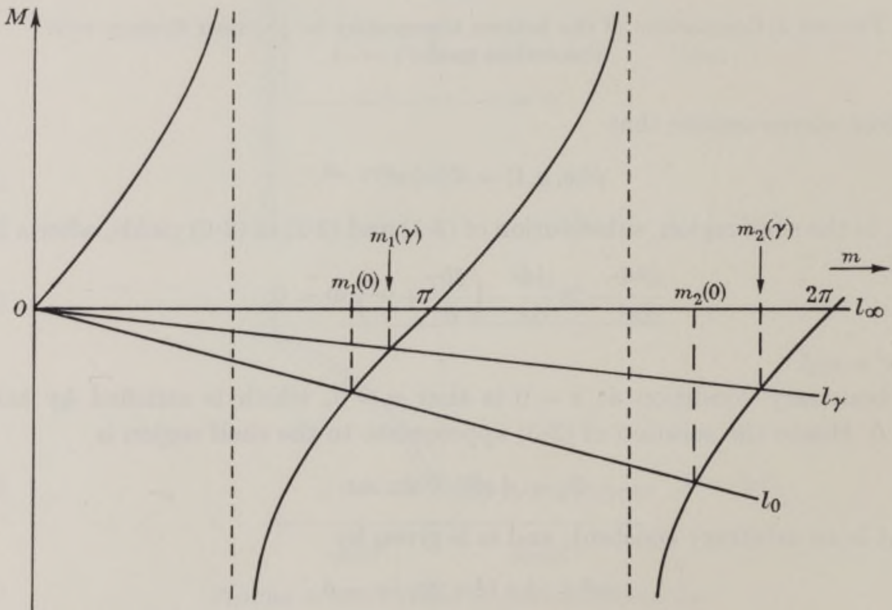

Figure 3. Intersections of $M = \tan m$ with $M = -m/(b+|\gamma|)$.

k is an integer. For $\gamma = 0$, l_0 has the equation $M = -m/b$. Denote the intersections of l_0 with the graph of $\tan m$ by $m_k(0)$, where the integer k denotes the appropriate branch of $\tan m$. Clearly $m_k(0) \to (k-\frac{1}{2})\pi$, as $k \to \infty$. As is illustrated in figure 3, for each value of γ there is an infinite number of intersections of l_γ with $\tan m$ at $m = m_k(\gamma)$, and $(k-\frac{1}{2})\pi < m_k(0) \leqslant m_k(\gamma) \leqslant k\pi$. Hence $m = m_k(\gamma)$ is a continuous function of $|\gamma|$, increasing monotonely from $m_k(0)$ to $k\pi$ as $|\gamma|$ varies from 0 to ∞. For instance, for $b = 2·7$ the approximate value of $m_1(0)$ is 2·4, so that $m_1(\gamma$ increases from 2·4 to π as $|\gamma|$ varies from 0 to ∞.

Now write equation (3·5) in the form

$$\sigma_k = \frac{-2b\gamma}{\gamma^2 + m_k^2 + b^2}, \tag{4·1}$$

where $m_k(\gamma)$ is that branch of the solution of (3·10) which tends to $k\pi$ as $|\gamma| \to \infty$. Now m_k is bounded above and below, so that $\sigma_k \sim -2b\gamma^{-1}$, as $|\gamma| \to \infty$, and

$$\sigma_k \sim \frac{-2b\gamma}{m_k^2(0) + b^2}, \tag{4·2}$$

as $\gamma \to 0$. Each value of k denotes a different branch of the function $\sigma(\gamma)$, in which $|\gamma|$ ranges from 0 to ∞. We shall call this the 'kth mode' of the shelf waves.

It is clear from (4·2) that for very long waves, σ_k is approximately linear in γ, and there is little dispersion. The phase and group velocities are nearly constant and equal to

$$-2bf/(m_k^2(0) + b^2).$$

For instance, using the Sydney profile in figure 2, then, to two significant figures, $b = 2{\cdot}7$ and $m_1(0) = 2{\cdot}4$. Also, locally $f = -\pi \sin 35^\circ$ rad/day. Hence, in the limit, the local velocity of long shelf waves is 240 km/day, or 280 cm/s, northwards.

From the behaviour of σ_k as $|\gamma| \to 0$, and as $|\gamma| \to \infty$, it may be inferred that the graph of $\sigma_k(\gamma)$ has a maximum, and also a point of inflexion. These can be located approximately by assuming that m_k is only a slowly varying function of γ, so that $m_k'(\gamma)$ is small. We may then differentiate (4·1) with respect to γ, keeping m_k constant, whence it follows that, approximately,

$$|\sigma_k^*| \approx \frac{b}{\sqrt{(b^2 + m_k^2)}}; \quad |\gamma_k^*| \approx \sqrt{(b^2 + m_k^2)}; \quad |\sigma_k^* \gamma_k^*| = b; \tag{4·3}$$

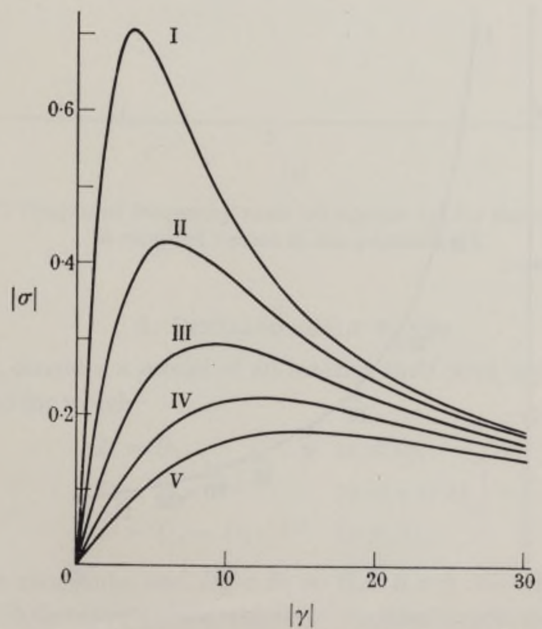

FIGURE 4. Graph of frequency ratio $|\sigma| = |\omega/f|$ against $|\gamma|$ for the first five modes of shelf waves in the case $b = 2{\cdot}7$.

where (σ_k^*, γ_k^*) are the coordinates of the maximum, and m_k takes some value between the limits $m_k(0)$ and $k\pi$. For values of $\gamma < \gamma_k^*$, the group velocity $c_g = \mathrm{d}\omega/\mathrm{d}\gamma$ has the same sign as the phase velocity $c_p = \omega/\gamma$, but if $\gamma > \gamma_k^*$, c_g and c_p have

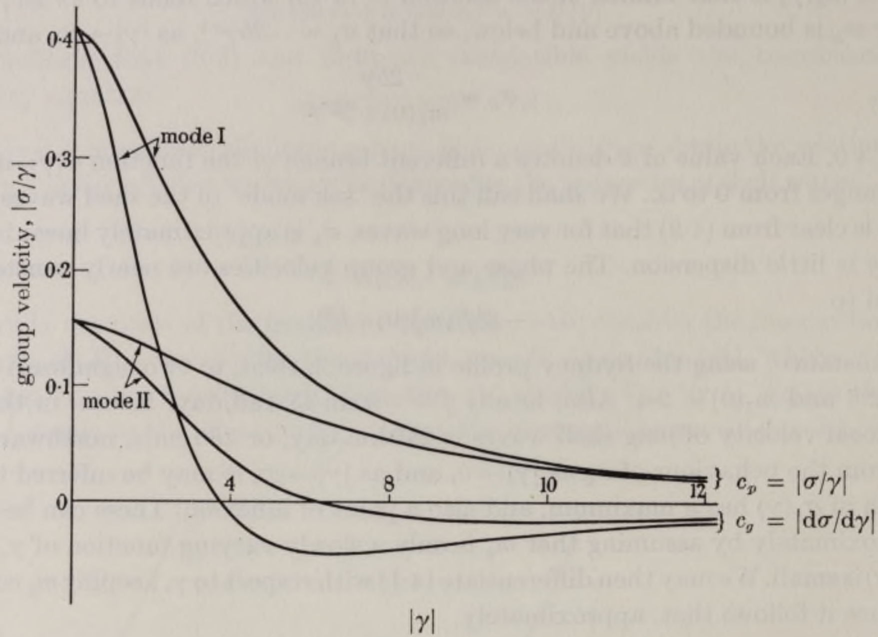

FIGURE 5. Graph of group velocity c_g and phase velocity c_p plotted against $|\gamma|$ for modes I and II of shelf waves.

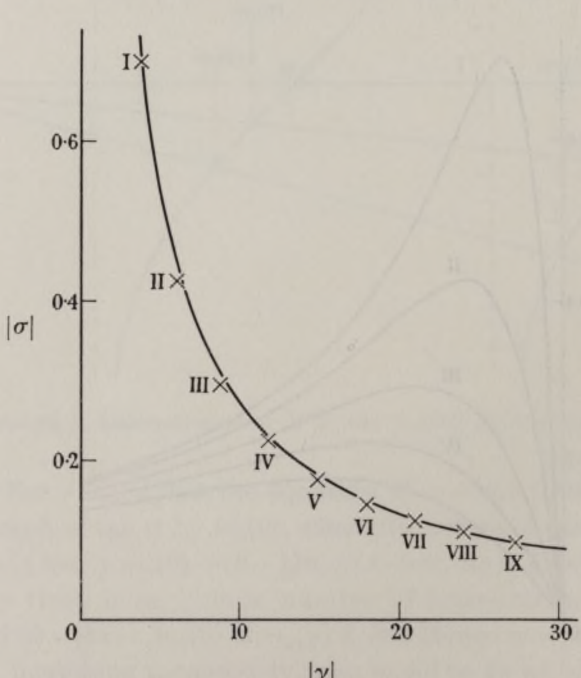

FIGURE 6. Comparison of points of zero group velocity in each mode, denoted by ×, with the approximating curve $|\sigma\gamma| = b$.

opposite sign. The group velocity has a turning point at the point of inflexion of $\sigma_k(\gamma)$, which is at $\gamma = \gamma_k^{**}$, given approximately by

$$\gamma_k^{**} \approx \sqrt{[3(b^2+m_k^2)]}.$$

These features are illustrated in figures 4 to 6 when $b = 2{\cdot}7$. The graph of $\sigma_k(\gamma)$ is given in figure 4 for the first five modes, and in figure 5 the phase velocity c_p and group velocity c_g are plotted against $|\gamma|$. Figure 6 shows how close the maxima of σ_k are to the approximate curve $\sigma_k^* \gamma_k^* = 2{\cdot}7$. In figure 7, $\sigma_1(\gamma)$ is plotted against $|\gamma|$ for different values of b.

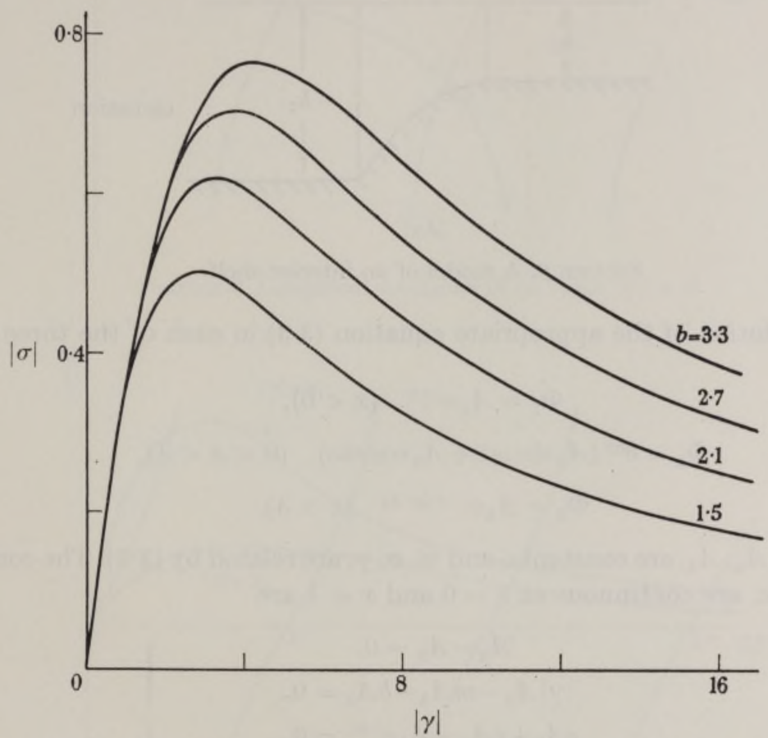

FIGURE 7. Graphs of frequency ratio $|\sigma|$ against $|\gamma|$ for the first mode, for a range of values of the parameter b.

5. Interior shelf waves

As in figure 8, consider a model of an interior shelf with a profile which is independent of y, and for which

$$\left.\begin{array}{ll} D = D_1 & (x \leqslant 0), \\ D = D_1\,\mathrm{e}^{-2bx} & (0 \leqslant x \leqslant \lambda), \\ D = D_2 = D_1\,\mathrm{e}^{-2b\lambda} & (x \geqslant \lambda), \end{array}\right\} \qquad (5{\cdot}1)$$

where D_1, D_2 are constants, and $D_2 < D_1$ so that $b > 0$. We denote by ψ_1, ψ_2, the streamfunctions in the appropriate regions of constant depth, and by ψ_s the streamfunction in the region $0 < x < \lambda$. Then, writing ψ in the form

$$\psi(x, y, t) = \Phi(x)\,\mathrm{e}^{\mathrm{i}(\gamma y - \omega t)}, \qquad (5{\cdot}2)$$

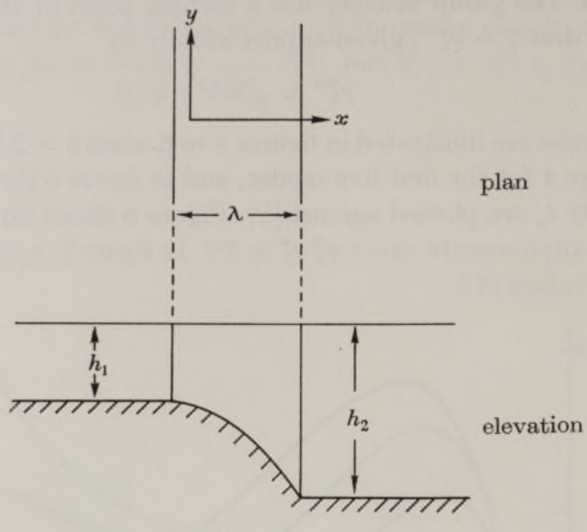

$|\lambda\gamma|$

FIGURE 8. A model of an interior shelf.

as in (3·2), solution of the appropriate equation (3·3) in each of the three regions yields

$$\Phi_1 = A_1 e^{|\gamma|x} \quad (x < 0), \tag{5·3}$$

$$\Phi_2 = e^{bx}(A_2 \sin mx + A_3 \cos mx) \quad (0 < x < \lambda), \tag{5·4}$$

$$\Phi_3 = A_4 e^{-|\gamma|(x-\lambda)} \quad (x > \lambda), \tag{5·5}$$

where A_1, A_2, A_3, A_4, are constants, and m, σ, γ, are related by (3·5). The conditions that Φ, $d\Phi/dx$, are continuous at $x = 0$ and $x = \lambda$ are

$$\left.\begin{aligned} A_1 - A_3 &= 0, \\ |\gamma| A_1 - mA_2 - bA_3 &= 0, \\ sA_2 + cA_3 - A_4 e^{-b\lambda} &= 0, \\ (bs+mc)A_2 + (bc-ms)A_3 + |\gamma| A_4 e^{-b\lambda} &= 0, \end{aligned}\right\} \tag{5·6}$$

where $s = \sin \lambda m$, and $c = \cos \lambda m$.

The condition that the equations (5·6) have a non-trivial solution is that

$$\tan \lambda m = \frac{2m|\gamma|}{m^2 + b^2 - \gamma^2}. \tag{5·7}$$

Let l_γ be the graph of the right-hand side of (5·7). In the case $\gamma^2 = b^2 + \delta^2 > b^2$, l_γ has an asymptote at $m = \delta$, as sketched in figure 9. It is obvious from the sketch that for $|\gamma| \geqslant b$ there is just one solution of (5·7) in each interval $(k-1)\pi < \lambda m \leqslant k\pi$, and for $\gamma = b$ all these intersections are at $\lambda m < (k-\frac{1}{2})\pi$, where $k = 1, 2, 3$, etc. A sketch of l_γ for $|\gamma| < b$ is given in figure 10, and it may be seen that, combining the two cases, for $k \geqslant 2$, $\lambda m_k(\gamma)$ varies monotonely from $(k-1)\pi$ to $k\pi$, as $|\gamma|$ varies from 0 to ∞. Thus for the second and higher modes, at any rate, the argument following (4·1) can be used to show that the shapes of the dispersion curves are much the same as in §4.

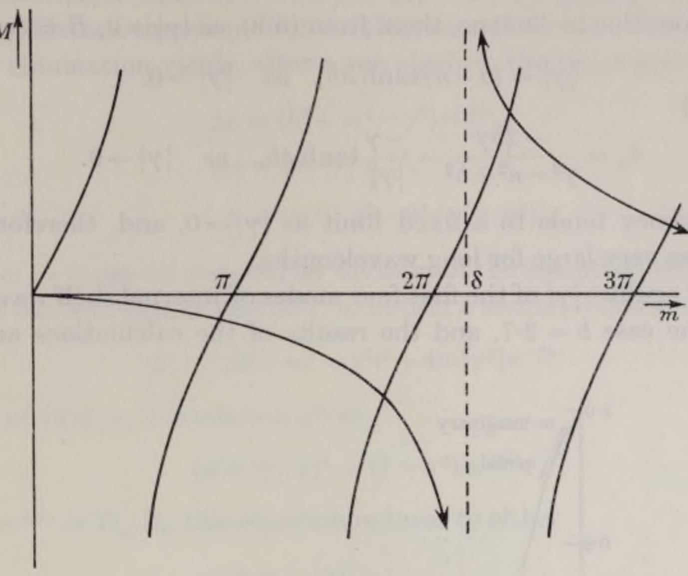

FIGURE 9. Graphical solutions of (5·7) for $|\gamma| > b$.

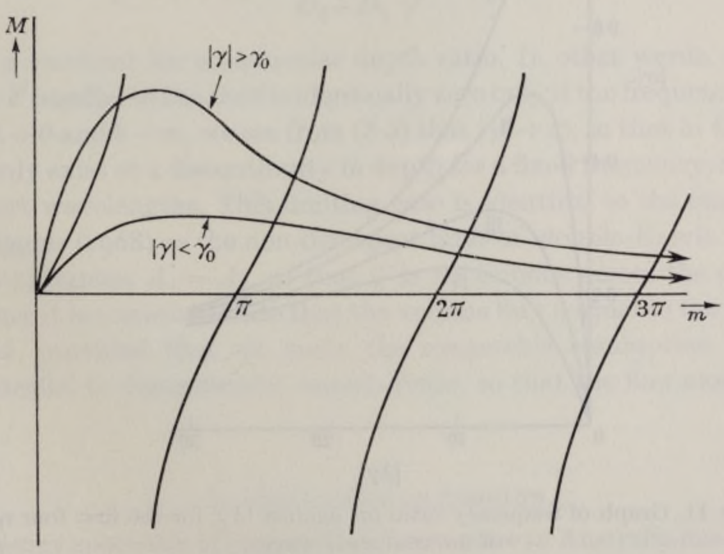

FIGURE 10. Graphical solutions of (5·7) for $|\gamma| < b$.

The first mode shows a rather different behaviour. It is easily verified that when $m = 0$, $\lambda|\gamma| = \sqrt{(1+\lambda^2b^2)}-1 = \lambda\gamma_0$ so that this value of $|\gamma|$ is the minimum that occurs for real m. However, put $m = in$, when (5·7) changes to

$$\tanh \lambda n = \frac{2n|\gamma|}{b^2-\gamma^2-n^2}, \tag{5·8}$$

and this equation has a root for n in the range $0 \leqslant n < b$, if and only if $\gamma_0 \geqslant |\gamma| \geqslant 0$. Thus the first mode does cover the full range of $|\gamma|$, but m is imaginary when $|\gamma| < \gamma_0$. The shapes of the dispersion curves are also somewhat modified. The only possibility of satisfying (5·8) when $|\gamma| \to 0$ is that $(b-n) \to B|\gamma|$, where B is some constant. Suppose this to be true, then, from (5·8), as $|\gamma| \to 0$, $B = \coth \lambda b$, so that

$$|\gamma| = (b-n)\tanh \lambda b, \quad \text{as} \quad |\gamma| \to 0.$$

Now, from (4·1)

$$\sigma_1 = \frac{-2b\gamma}{\gamma^2 - n^2 + b^2} \to \frac{-\gamma}{|\gamma|}\tanh \lambda b, \quad \text{as} \quad |\gamma| \to 0.$$

Thus, the frequency tends to a fixed limit as $|\gamma| \to 0$, and, therefore, the phase velocity becomes very large for long wavelengths.

The graphs σ against $|\gamma|$ of the first four modes of internal shelf waves have been computed in the case $b = 2·7$, and the results of the calculations are plotted in figure 11.

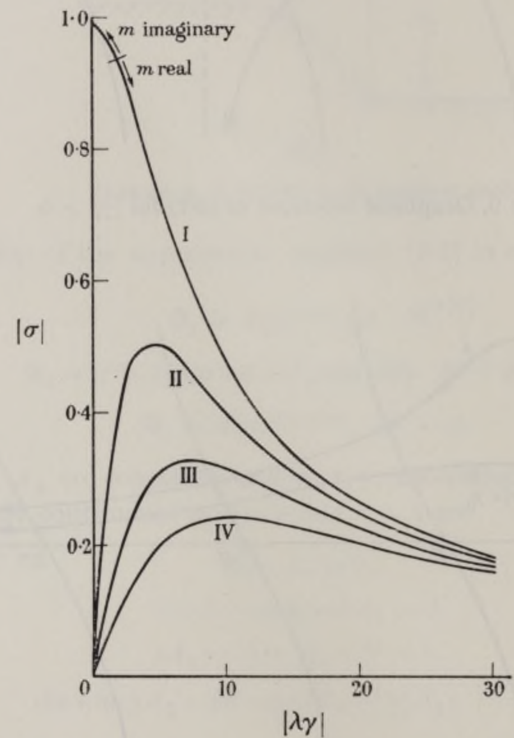

Figure 11. Graph of frequency ratio $|\sigma|$ against $|\lambda\gamma|$ for the first four modes of internal shelf waves.

There remains the question of what happens as $\lambda \to 0$, $b \to \infty$, with $\lambda b = \frac{1}{2}\ln(D_1/D_2)$ kept constant, so that the shelf tends to an abrupt step. Now the volume flux parallel to the shelf is given by

$$F = \int_0^\lambda \{v/D\}\,\mathrm{d}x = \int_0^\lambda \frac{\partial \psi}{\partial x}\,\mathrm{d}x,$$
$$= [\Phi_2]_0^\lambda \, \mathrm{e}^{\mathrm{i}(\gamma y - \omega t)},$$
$$= [(sA_2 + cA_3)\,\mathrm{e}^{b\lambda} - A_3]\,\mathrm{e}^{\mathrm{i}(\gamma y - \omega t)}.$$

If infinite velocities are impossible, then $F \to 0$ as $\lambda \to 0$, so that, in the limit,

$$sA_2 + cA_3 = A_3\,\mathrm{e}^{-b\lambda}. \tag{5·9}$$

When this equation is combined with the first and third of (5·6), it follows that $A_1 = A_3 = A_4$. The last three equations of (5·6) are now in the two unknowns A_2, A_3, so that their elimination yields, after some algebra, the two equations

$$\left.\begin{aligned}\Delta c &= (b^2+m^2-\gamma^2)\,\mathrm{e}^{-b\lambda},\\ \Delta s &= 2m\,|\gamma|\,\mathrm{e}^{-b\lambda},\end{aligned}\right\} \qquad (5\cdot10)$$

where $$\Delta = (m^2+b^2-2b\,|\gamma|+\gamma^2).$$

The relation (5·7) can be deduced by division of the second equation by the first. However, we can also square and add, to obtain a second relation of the form

$$\Delta^2 = [(b^2+m^2-\gamma^2)^2+4m^2\gamma^2]\,\mathrm{e}^{-2b\lambda}. \qquad (5\cdot11)$$

Substitution of (3·5) in this relation gives

$$(\sigma+|\gamma|/\gamma)^2 = (1-\sigma^2)\,\mathrm{e}^{-2b\lambda}.$$

Noting that $\mathrm{e}^{-2b\lambda} = D_2/D_1$, this equation reduces to either

$$\sigma = -|\gamma|/\gamma,$$

or $$\sigma = \frac{D_2-D_1}{D_2+D_1}\frac{|\gamma|}{\gamma} = \sigma_0,$$

where σ_0 is a constant for a particular depth ratio. In other words, the resultant volume flux F parallel to the shelf is identically zero only if the frequency is constant.

Now, as $\lambda \to 0$ and $b \to \infty$, we see from (3·5) that $|\gamma| \to \infty$, so that in the limit, shelf waves can only exist at a discontinuity in depth for a fixed frequency, and then only for very short wavelengths. This limiting case is identical to the one deduced by Longuet-Higgins (1968) as the non-divergent limit of 'double-Kelvin' waves. Note also that (5·9) implies $A_1 = A_4$, so that ψ is continuous across the depth discontinuity. Hence it is correct to state that the volume flux normal to the discontinuity is conserved, provided that we make the reasonable assumption that particle velocities parallel to discontinuity remain finite, so that the flux along the step is zero.

6. Discussion of results

The frequency spectrum of the barometric pressure in Australia has a broad peak at a period of 5 to 9 days depending on the season. For Sydney, therefore, we are looking for a response in sea level to generating forces which have a frequency ratio σ of about 0·15. As can be seen from figure 4, the corresponding wavelengths in the first mode are 1500 km, and 11·5 km. The latter are out of the question because of dissipation, and it is reasonable to conclude that for Hamon's observations a linear model of the first mode or two such as given by Robinson's theory is probably sufficient. However, this is not so for shorter periods—for instance at periods of 2 to 3 days it would be necessary to look for the shorter waves whose energy travels southwards, as well as the longer waves whose energy propagates to the north. In particular, the zero group velocity is very noteworthy. At the corresponding periods in the respective modes the energy cannot move away from the point of application of a forcing disturbance, and a form of resonance occurs. The actual significance of this interesting phenomenon awaits both experimental and theoretical verification, the latter in a model which takes both generating forces and friction into account.

The turning point in the group velocity in each mode could also be worth further investigation. As is well known (Jeffreys & Jeffreys 1946, p. 476), such a turning point corresponds to the 'Airy phase', and may be observationally significant, particularly as the corresponding wavelengths are comparatively short.

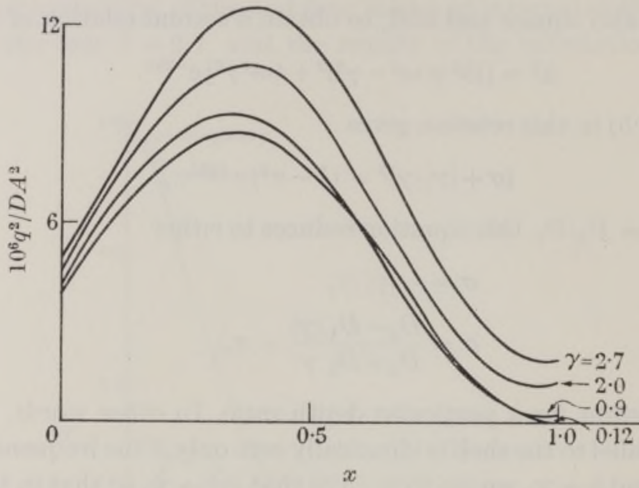

FIGURE 12. Profile for the first mode of energy density $E \propto q^2/D$, where q is the mean particle velocity, across the continental shelf, for various values of $|\gamma|$. Note that for small values of $|\gamma|$, E is small when $x = 1$, i.e. at the edge of the shelf.

The actual trapping mechanism is also interesting. For short waves it is obvious from (3·6), (5·3) and (5·5) that amplitudes in the ocean decay rapidly with distance from the shelf, so that energy is trapped in the shelf region. However, this cannot be true for the very long waves, because the amplitude decay in the ocean is far too slow to give a satisfactory explanation of trapping. What actually happens for very long waves is that from (2·5), $v \gg u$ in the shelf region. However, in regions of constant depth, v and u must be of the same order of magnitude. Hence at the edge of the shelf v must be much less than in the interior. For instance, in equations (3·9) and (3·10), if $|\gamma| \ll b$, then the approximation

$$\tan m = -m/b$$

to (3·10) can be obtained by using the condition $v(1) = 0$, instead of the continuity conditions (3·7). Figure 12 shows how the energy density varies across the shelf for different values of γ. It can be seen that if $|\gamma|$ is small the energy density is almost zero at the edge of the shelf, so that energy is trapped in the region despite the slow rate of amplitude decay in the ocean.

There remains the vital question of what generates shelf waves. In view of the high correlation between adjusted sea levels and barometric pressure in Hamon's observations, it is reasonable to look for a forcing mechanism directly dependent on pressure. If pressure forcing terms are put into the equations of motion (2·1) and (2·2), then it turns out in the non-divergent case that the forcing terms cancel in deriving the vorticity equation (2·6). Consequently the small parameter ϵ must be a factor in the pressure forcing terms, and the response to variations in barometric pressure cannot be measurably different to that predicted by the isostatic theory. It has been suggested by Myzak (1967) that the observed response is due to resonance of shelf waves as they travel round the coast of Australia. This must imply that shelf waves repeatedly travel the full circumference of the continent, and reinforce sufficiently to cancel both dissipation and the ϵ factor. It appears most unlikely that such reinforcement as this can occur even under favourable circumstances, but it is our opinion that the presence of New Guinea linked to Australia by the shallow Torres straits must block east coast shelf waves from reaching the west coast even once. Further supporting evidence is provided by the apparent absence of shelf waves at Hobart, indicating that the observations on the east coast can only be explained by purely local generating forces.

An alternative theory put forward by the authors is that the observations are due to the response of the shelf to the stress due to the longshore component of the geostrophic wind. The present of the shelf implies that the mean current generated by the wind is greater in the shallower water. It can be shown that, for a geostrophic wind with a maximum velocity as small as 10 knots, the vorticity generated on the shelf gives rise to changes in sea level of the same sign and order of magnitude as those actually observed. We hope to be able to present this theory in a subsequent publication.

Appendix

If the y axis points north, and $\partial f/\partial y = \beta$, then in the non-divergent case the vorticity equation similar to (2·6) is

$$\frac{\partial}{\partial t}\left[\frac{\partial}{\partial x}\left(D\frac{\partial\psi}{\partial x}\right)+\frac{\partial}{\partial y}\left(D\frac{\partial\psi}{\partial y}\right)\right]+f\left(\frac{\partial D}{\partial y}\frac{\partial\psi}{\partial x}-\frac{\partial D}{\partial x}\frac{\partial\psi}{\partial y}\right)+\beta D\frac{\partial\psi}{\partial x}=0. \tag{A 1}$$

When $D = D_0\,e^{-2bx}$, and $\psi = \Phi(x)\,e^{i(\gamma y-\omega t)}$, then, instead of (3·3) we have

$$\frac{d^2\Phi}{dx^2}+\left(\frac{i\beta}{\omega}-2b\right)\frac{d\Phi}{dx}-\left(\frac{2b\gamma}{\sigma}+\gamma^2\right)\Phi=0. \tag{A 2}$$

Typical values of the constants are $b = 2{\cdot}7, f/\omega = 8, \beta/f = R^{-1}\cot\theta$, where R is the radius of the earth, and $\theta \approx 35°$. Hence, for these values $|\beta/2b\omega| \approx 3\times10^{-2}$, and, within the limits of accuracy of the model, we may take $\beta = 0$ in the shelf region. However, in the ocean $b = 0$ and (A 2) reduces to

$$\frac{d^2\Phi}{dx}+\frac{i\beta}{\omega}\frac{d\Phi}{dx}-\gamma^2\Phi=0, \tag{A 3}$$

so that (3·6) changes to

$$\Phi_0 = \beta\,e^{-\alpha(x-1)}, \tag{A 4}$$

where $\alpha = i\rho+\sqrt{(\gamma^2-\rho^2)}$, and $\rho = \beta/2\omega$.

Equation (3·10) changes to

$$\tan m = -m/(b+\alpha). \tag{A 5}$$

As before, $|\rho/b| \ll 1$, so that, independently of the relative magnitudes of ρ and γ, α may be replaced by $|\gamma|$ in (A 5). Hence we may neglect the term in β in (A 1), and therefore, the f-plane approximation is valid for the time and length scales considered in this paper.

References

Hamon, B. V. 1962 The spectrums of mean sea level at Sydney, Coffs Harbour, and Lord Howe Island. *J. Geophys. Res.* **67**, 5147–5155.

Hamon, B. V. 1963 Corrections to: The spectrums of mean sea level at Sydney, Coffs Harbour and Lord Howe Island. *J. Geophys. Res.* **68**, 4635.

Hamon, B. V. 1966 Continental shelf waves and the effects of atmospheric pressure and wind stress on sea level. *J. Geophys. Res.* **71**, 2883–2896.

Jeffreys, H. & Jeffreys, B. S. 1946 *Methods of mathematical physics*. Cambridge University Press.

Longuet-Higgins, M. S. 1964 Planetary waves on a rotating sphere. *Proc. Roy. Soc.* A **279**, 446–473.

Longuet-Higgins, M. S. 1965 Planetary waves on a rotating sphere. II. *Proc. Roy. Soc.* A **284**, 40–54.

Longuet-Higgins, M. S. 1968 On the trapping of waves along a discontinuity of depth in a rotating sea. *J. Fluid Mech.* (in the Press).

Myzak, L. A. 1967 On the theory of continental shelf waves. *J. Mar. Res.* **25**, 205–227.

Robinson, A. R. 1964 Continental shelf waves and the response of sea-level to weather systems. *J. Geophys. Res.* **69**, 367–368.